

Supporting Information

Hydrogen Peroxide Generation at Liquid-liquid Interface under Conditions Unfavorable for Proton Transfer from Aqueous to Organic Phase.

Justyna Jedraszko^a, Wojciech Nogala^a, Wojciech Adamiak^a, Ewa Rozniecka^a, Iwona Lubarska-
Radziejewska^a, Hubert Girault^b, Marcin Opallo*^a

a/ Institute of Physical Chemistry, Polish Academy of Sciences, Warsaw, Poland

b/ LEPA, Ecole Polytechnique Federale de Lausanne, Lausanne, Switzerland

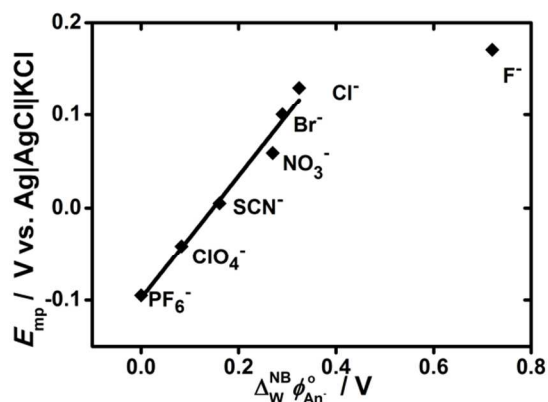


Figure S1. Dependence of the mid-peak potential of DMFc⁺/DMFc couple, E_{mp} , (obtained from the data presented on Fig.2) on the standard transfer potential of studied anions, $\Delta_W^{NB} \phi_{An}^o$ ^{2,17}. The GC electrode was coated with 2 μL of 1 mol dm^{-3} DMFc in 0.1 mol dm^{-3} THxAP in DCE and immersed in 0.1 mol dm^{-3} aqueous solution of various anions. Scan rate: 50 mV s^{-1} .

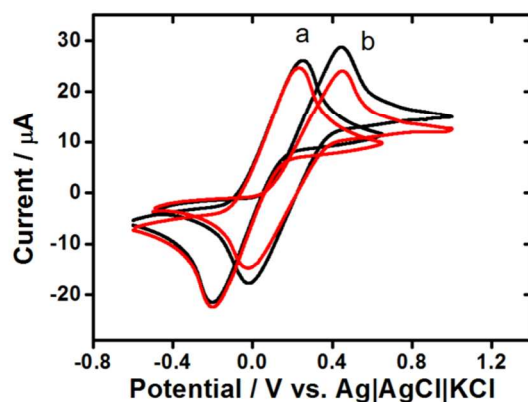


Figure S2. Cyclic voltammograms recorded at GC electrode immersed in 0.1 mol dm^{-3} aqueous solution of NaClO₄ (curves a) and NaCl (curves b). Black curve was 1st scan and red curve 2nd scan. The GC electrode was covered with 30 μL of 5 mol dm^{-3} DMFc solution in 0.1 mol dm^{-3} THxAP in DCE. Scan rate was 50 mV s^{-1} .

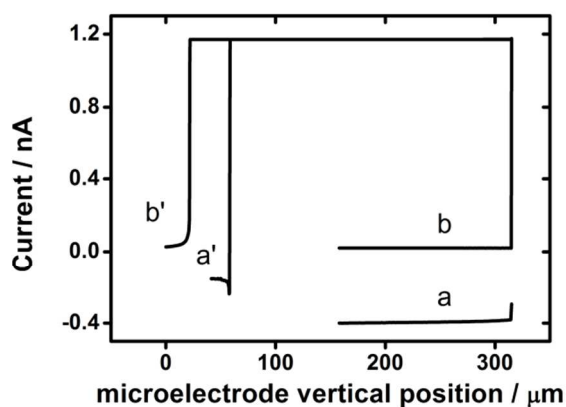


Figure S3. Approach curves (a, b) to liquid-liquid interface formed between droplet of 2 μL of 5 mmol dm^{-3} DMFc solution in 0.1 mol dm^{-3} THxAP in DCE deposited on GC electrode and 0.1 mol dm^{-3} aqueous of NaClO_4 (a) and NaCl (b). Tip potential: 0.2 V.. Curves (a') and (b') represent retractions for the same systems, respectively. Tip velocity: 1 $\mu\text{m s}^{-1}$.

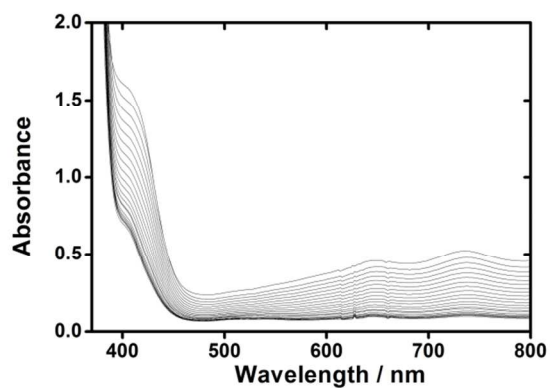


Figure S4. UV-vis spectra of solution obtained by mixing 1.4 mL of 0.5 g dm^{-3} HRP and 1.82 mmol dm^{-3} $\text{ABTS}(\text{NH}_4)_2$ solutions in 0.1 mol dm^{-3} phosphate buffer (pH 7) with 0.6 mL of 0.5 mol dm^{-3} aqueous HClO_4 . The spectra were recorded 60 s after addition of H_2O_2 . Range of H_2O_2 concentration: 0 - 74 mmol dm^{-3} .

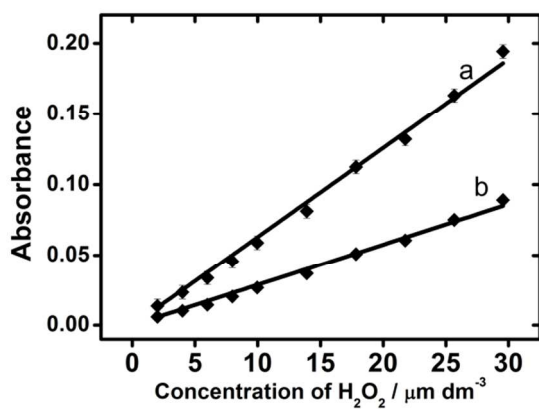


Figure S5. Calibration curves of absorbance vs. H₂O₂ concentration for two wavelengths: $\lambda=416$ nm (a) and 736 nm (b). The slopes are for curve a: $6293.55 \text{ dm}^3 \mu\text{mol}^{-1}$ ($R^2=0.998$) and b: $2875.03 \text{ dm}^3 \mu\text{mol}^{-1}$ ($R^2=0.997$).

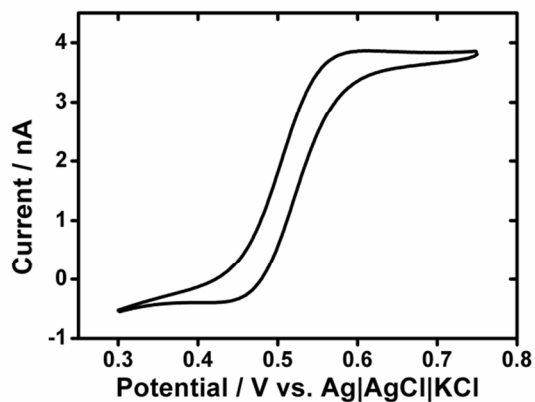


Figure S6. Cyclic voltammogram obtained at the Pt SECM tip (25 μm , diameter) for 0.5 g dm^{-3} HRP, $1.82 \text{ mmol dm}^{-3}$ (NH₄)₂ABTS in 0.1 mol dm^{-3} aqueous HClO₄. Scan rate 50 mV s^{-1}

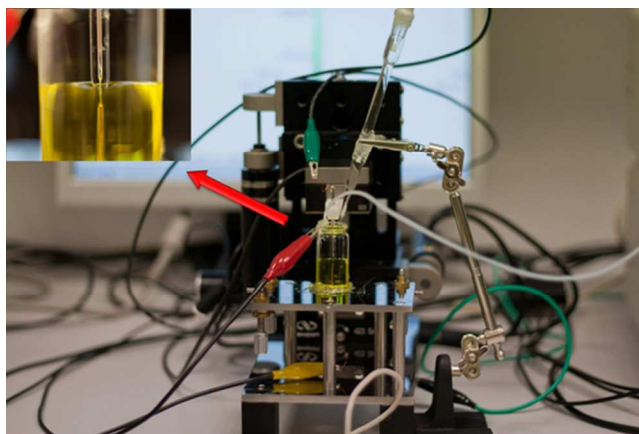


Figure S7. Photo of the experimental setup used for SECM experiment with two microelectrodes positioned close to liquid|liquid interface.

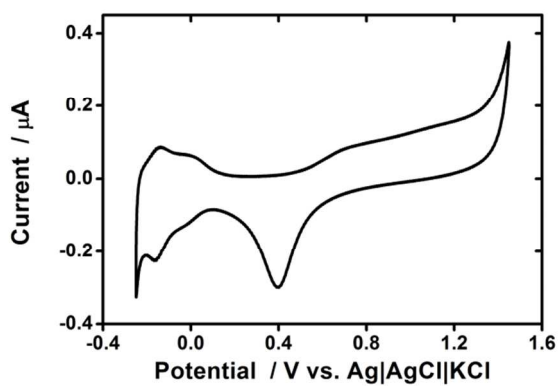


Figure S8. Cyclic voltammogram (2nd cycle) recorded at WE1 in $0.1 \text{ mol dm}^{-3} \text{ HClO}_4$ solution. Scan rate: 50 mV s^{-1} .

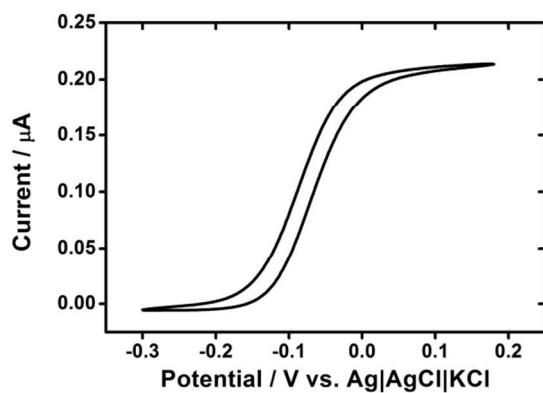


Figure S9. Cyclic voltammogram (2nd cycle) measured at WE2 for 10 mmol dm⁻³ DMFc with 0.1 mol dm⁻³ THxAP in DCE. Scan rate: 20 mV s⁻¹.

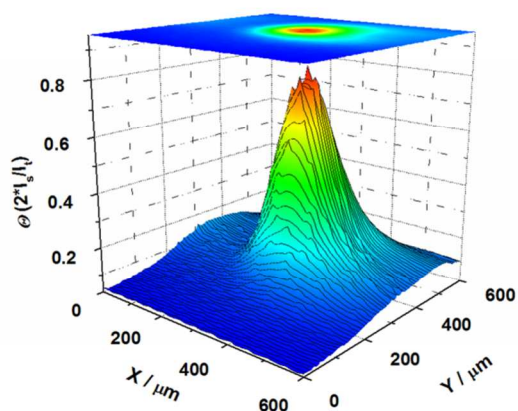


Figure S10. The dependence of the calculated collection efficiency on the tip position in the experiment presented in Figure 10.

Equation S1. Expression for the normalized tip current used for calculation of organic phase thickness:

$$\begin{aligned}
 & I_T(L, \kappa, RG) \\
 &= \left(\left(\ln 2 + \ln 2 \left(1 - \frac{2}{\pi} \cos^{-1} \left(\frac{1}{RG} \right) \right) - \ln 2 \left(1 - \left(\frac{2}{\pi} \cos^{-1} \left(\frac{1}{RG} \right) \right)^2 \right) \right) \right. \\
 &+ \frac{1}{2 \cdot \left(1 + 0.639 \left(1 - \frac{2}{\pi} \cos^{-1} \left(\frac{1}{RG} \right) \right) - 0.186 \left(1 - \left(\frac{2}{\pi} \cos^{-1} \left(\frac{1}{RG} \right) \right)^2 \right) \right) \left(\frac{2}{\pi} \tan^{-1} \left(L + \frac{1}{\kappa} \right) \right)} \\
 &+ \left. \left(1 - \left(\ln 2 + \ln 2 \left(1 - \frac{2}{\pi} \cos^{-1} \left(\frac{1}{RG} \right) \right) - \ln 2 \left(1 - \left(\frac{2}{\pi} \cos^{-1} \left(\frac{1}{RG} \right) \right)^2 \right) \right) \right) \right. \\
 &- \left. \frac{1}{2 \cdot \left(1 + 0.639 \left(1 - \frac{2}{\pi} \cos^{-1} \left(\frac{1}{RG} \right) \right) - 0.186 \left(1 - \left(\frac{2}{\pi} \cos^{-1} \left(\frac{1}{RG} \right) \right)^2 \right) \right) \left(\frac{2}{\pi} \tan^{-1} \left(L \right. \right. \right. \\
 &+ \left. \left. \left. \frac{1}{\kappa} \right) \right) \right) + \frac{\left(\frac{2.08}{RG^{0.358}} \left(L - \frac{0.145}{RG} \right) + 1.585 \right)}{\left(1 + 2.47RG^{0.31}L\kappa \right) \left(1 + L^{(0.006RG+0.113)}\kappa^{-(0.0236RG+0.91)} \right)} - 1
 \end{aligned}$$

$$\kappa = \frac{k_{eff} r_T}{D}$$

, where k_{eff} is heterogeneous rate constant, L is dimensionless tip-substrate distance, D is diffusion coefficient and r_T is radius of tip, RG is the ratio of the radius of the disk insulator and of the radius of electrode.

“This material is available free of charge via the Internet at <http://pubs.acs.org>.”